American Mineralogist, Volume 84, pages 754–763, 1999

Niobian rutile from the McGuire granitic pegmatite, Park County, Colorado: Solid solution, exsolution, and oxidation

PETR ČERNÝ ,[1,*] RON CHAPMAN,[1] WILLIAM B. SIMMONS,[2] AND LEONARD E. CHACKOWSKY[1]

[1] Department of Geological Sciences, University of Manitoba, Winnipeg, Manitoba R3T 2N2, Canada
[2] Department of Geology and Geophysics, University of New Orleans, New Orleans, Louisiana 70148-2850, U.S.A.

ABSTRACT

Coarse crystals of niobian rutile occur in the hydrothermally altered core-margin zone of the McGuire granitic pegmatite, Park County, Colorado, associated with potassium feldspar, quartz, biotite, ilmenite, and monazite-(Ce). Primary homogeneous niobian rutile, with Fe^{3+} Fe^{2+} and a small excess of (Fe,Mn) over the amount required to compensate the incorporation of (Nb,Ta,W), underwent three stages of exsolution. Primary homogeneous niobian rutile exsolved a fine trellis-like pattern of minor lamellar Nb-bearing pseudorutile I. Most of this phase was broken down to pseudomorphs consisting of microgranular Nb-rich pseudorutile II imbedded in niobian-ferrian "ferropseudobrookite." Continued exsolution in niobian rutile and reconstitution of the early exsolution products generated (Fe,Nb)-depleted, microgranular niobian rutile, titanian ferrocolumbite, and minor ilmenite. These three phases did not attain chemical equilibrium but may represent a stable phase assemblage. All these processes seem to have maintained charge balance, suggesting a closed system. Subsequent to the three stages of exsolution, extensive oxidation converted the mineral assemblages to anatase + hematite + titanian-tungstenian ixiolite; primary ilmenite was oxidized into an anatase + hematite intergrowth. In both cases, the hematite component was almost completely leached out, leaving highly porous aggregates of the other phases. The exsolution products in niobian rutile are controlled by the (Fe+Mn+Sc)/(Nb+Ta+W) ratio of the primary phase and by its $(Fe^{3+}+Sc)/(Fe^{2+}+Mn)$ ratio. Dominance of divalent A-cations facilitates exsolution of titanian ferro- to manganocolumbite or titanian ixiolite, whereas dominant trivalent cations lead to exsolution of titanian $(Fe,Sc)^{3+}NbO_4$ phases. Excess (Fe,Mn) over the columbite-type $Fe^{2+}Nb_2$ stoichiometry causes exsolution of (Fe,Mn)-rich Nb,Ta-oxide minerals or complementary (Fe,Mn,Ti) phases.

INTRODUCTION

Niobian and tantalian rutile, also known as ilmenorutile and strüverite, respectively, have been viewed as rare minerals, found only in a few categories of rare-element pegmatites. However, during the last three decades, they were recognized as significant accessory minerals in peraluminous to peralkaline granitic rocks, and as substantial components of hydrothermal assemblages associated with alkaline intrusions. They are economically important in several types of lithophile rare-element mineralization (Černý and Ercit 1985, 1989). However, the understanding of many aspects of these phases is still unsatisfactory. In particular, niobian rutile with substantial contents of Nb is unstable at low temperatures: niobian rutile with Fe^{2+} distinctly dominant over Fe^{3+} exsolves titanian columbite or ixiolite, while the rutile matrix becomes impoverished in Nb, Ta, Fe, and Mn (e.g., Černý et al. 1964, 1981, 1986; Sahama 1978; M. Leroux et al., unpublished experimental data). A recent study of niobian rutile with Fe^{3+} Fe^{2+} revealed exsolution of a $(Fe^{3+},Sc)(Nb,Ta)O_4$-dominant phase, not yet defined as a mineral species (Černý and Chapman, unpublished manuscript). This work prompted further examination of niobian rutile of diverse primary compositions. The present study describes a case of niobian rutile with Fe^{2+} Fe^{3+}, which breaks down into three secondary minerals with five different compositions with subsequent extensive oxidation.

This study is dedicated to the memory of our colleague and friend, Gene Foord, whose lifelong work contributed so much to our understanding of Nb,Ta-bearing minerals.

THE PARENT PEGMATITE

The niobian rutile occurs in the McGuire pegmatite, one of the outlying bodies of the South Platte pegmatite district, Jefferson County, Colorado (Simmons and Heinrich 1980; Simmons et al. 1987). The south Platte pegmatite population is a typical representative of the NYF-family pegmatites, derived from a quartz monzonite in the northern termination of the Pikes Peak batholith (cf. Černý 1991, 1992 for pegmatite classification). The McGuire pegmatite is located in the adjacent Park County, 16 km southwest of the central cluster of the South Platte pegmatites and 6 km northwest of Wellington Lake

*E-mail: p_cerny@umanitoba.ca

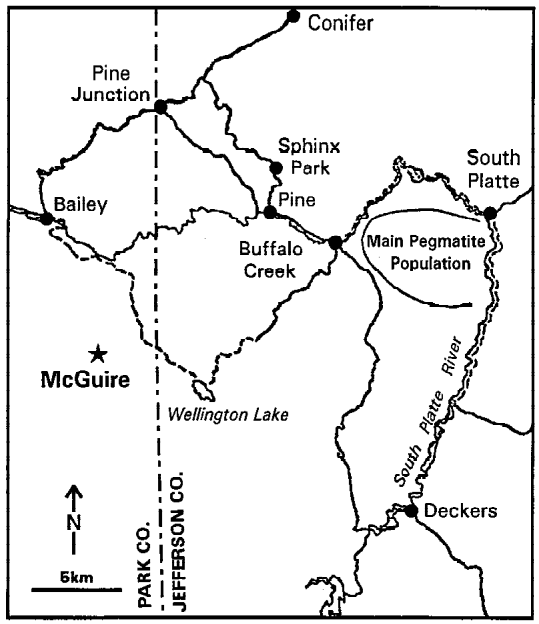

FIGURE 1. Location of the McGuire pegmatite, Park County, Colorado with respect to the main population of the South Platte pegmatites (centered at about 105°12'30" W, 39°22'30" N); modified after Simmons et al. (1987).

(Fig. 1). The pegmatite is 40 by 60 m in surface plan section, consists of a narrow wall zone with quartz, microcline-perthite, and biotite, and has an unsegregated blocky core of microcline perthite and quartz. Most of the core was removed by mining for feldspar in the 1950s.

The occurrence of niobian rutile is restricted to a small area in the northwestern side of the pegmatite. Niobian rutile is associated with microcline-perthite, quartz, biotite, ilmenite, and monazite-(Ce). The microcline-perthite is extensively albitized, sericitized, and heavily stained by Fe oxides. In addition, the Ti-oxide minerals also show profound hydrothermal alteration.

Because most of the above assemblage was recovered from material slumped from the quarry wall, it was not possible to ascertain its precise paragenetic position. However, the assemblage is located in a core-margin zone, at the boundary of the wall zone and the blocky core in what is inferred to be the hinge of a small roll in the pegmatite, marked by a small outcrop of granite exposed in the floor of the quarry. The assemblage seems to be a primary component of the inward crystallization of the pegmatite from the wall zone into the core margin. Replacement and alteration, however, are at least in part superimposed on the primary assemblage.

EXPERIMENTAL AND TERMINOLOGY

The examined minerals were analyzed using the Cameca SX-50 electron microprobe in wavelength-dispersion mode, under conditions given by Novák and Černý (1998). To facilitate mutual comparison of chemical compositions of rutile, titanian columbite, ixiolite, and anatase, the cation contents of all four phases are normalized to eight atoms of oxygen. This gives atomic content per unit cell (apuc) for ixiolite and disordered columbite, and per two unit cells (ap2uc) of rutile and anatase. Cation contents of other phases are given per formula unit (apfu) or per two formula units (ap2fu). Normalization to a given number of oxygen atoms was in all cases constrained to the maximum number of cations permitted by the structure, which was maintained by conversion of appropriate amount of Fe^{2+} to Fe^{3+}. The legitimacy of calculated Fe^{3+} was established by Ercit (1986) and Ercit et al. (1992) on the example of wodginite samples examined by Mössbauer spectroscopy. The differences between the Mössbauer data and the calculated values did not exceed 10% Fe_2O_3 relative and were largely less than 5%. The relative error would rapidly increase with decreasing total Fe and with decreasing proportion of Fe^{3+}. In the present study, the total Fe content is substantial in all minerals examined and so is that of Fe_2O_3. Consequently, the relative error of calculated ferric iron should not exceed 10%. The sole exception is ilmenite, particularly the DIL type depleted in A cations. As discussed later, the fine compositional details of this phase remain uncertain.

Unit-cell dimensions were refined from X-ray powder-diffraction data, collected on the Philips 1710 automated powder diffractometer. Annealed CaF_2 with a = 5.46379(4) Å, calibrated against a NBS silicon reference (batch 640; a = 5.430825 Å), was used as an internal standard. Refinements were done using the FIX program for reduction of systematic error in positional data of X-ray powder-diffraction maxima to ±0.01° 2θ (Ercit 1986), and a modified version of the CELREF least-squares program of Appleman and Evans (1973).

The term exsolution is used here in its broadest sense, as the specific relationships between the different pairs of products cannot be established. Textural and crystal-structural relationships suggest semi-coherent exsolution of pseudorutile from niobian rutile, but incoherent style is probably typical of other cases (cf. Putnis 1992, p. 335–336 and 342–343 for hierarchy of homogeneous exsolution products).

NIOBIAN RUTILE

Niobian rutile forms black subhedral platy crystals up to 6 cm long, indistinguishable in hand specimen from the associated ilmenite. Optical examination in reflected light and backscattered-electron images (BSE) show that the primary homogeneous rutile phase underwent two exsolution processes, followed by oxidation.

Early exsolution: niobian pseudorutile I, II, and niobian "ferropseudobrookite"

Only small microscopic patches of the early exsolution assemblage are locally preserved, consisting of a rutile phase crisscrossed by a trellis-like network of exsolution products (Fig. 2A). Although the identity of rutile is confirmed by X-ray diffraction, the structural aspects of the exsolution products cannot be examined by routine methods. Thus, interpretation of the chemical composition and identification of the exsolved minerals are based on formula normalizations giving the best weight percent totals, integral cation-oxygen ratios, and realistic Fe^{3+}/Fe^{2+} ratios. As discussed under crystal chemistry, the choice always converges in a single candidate, and the mineral identities can be taken as well established.

TABLE 1. Representative composition of the McGuire niobian rutile and its exsolution products

	R1	R2	PRI1	PRI2	PRII1	PRII2	PB1	PB2	RU1	RU2	C1	C2	ILM
WO_3	1.80	1.63	1.83	1.60	2.02	2.13	0.72	0.57	0.06	–	6.43	8.63	0.30
Nb_2O_5	27.60	27.70	26.00	26.50	28.70	34.80	18.40	13.90	14.40	8.12	57.70	55.80	0.77
Ta_2O_5	4.42	4.39	3.43	3.63	4.54	4.69	2.17	1.70	4.74	3.69	4.52	3.79	–
TiO_2	51.70	51.33	34.10	36.10	32.43	26.83	38.60	40.83	70.90	81.50	7.49	8.78	51.10
ZrO_2	0.12	0.17	0.23	0.18	0.17	0.27	0.06	0.06	–	–	0.96	0.86	–
SnO_2	0.73	0.89	0.47	0.68	0.85	0.52	0.26	0.24	1.07	0.62	1.13	0.89	–
UO_2	–	–	–	0.18	–	–	0.19	–	–	–	–	–	–
Sc_2O_3	0.11	0.18	0.31	0.16	0.21	0.46	0.19	0.07	0.04	–	0.50	0.72	–
Y_2O_3	–	0.04	0.02	–	–	0.01	–	–	–	–	0.06	0.01	–
Sb_2O_3	0.05	–	–	–	–	–	–	0.06	–	–	–	–	–
Bi_2O_3	–	0.06	–	–	–	–	–	0.09	–	0.12	–	0.14	–
Fe_2O_3	7.21	7.39	17.83	14.01	12.09	8.01	10.03	14.94	5.49	4.01	4.00	4.71	1.03
FeO	5.33	5.25	14.76	17.11	18.04	20.70	24.98	20.56	2.15	0.87	15.70	15.48	46.76
MnO	0.02	0.03	0.95	0.64	0.97	1.27	3.80	4.78	–	0.06	0.50	0.07	0.73
CaO	–	0.01	–	–	0.03	0.01	0.03	0.03	0.01	–	0.02	–	–
MgO	–	–	0.01	–	–	0.02	0.02	–	–	–	–	–	0.02
ZnO	0.11	–	–	–	–	–	–	–	–	0.05	–	–	–
PbO	–	–	–	–	–	–	–	0.09	0.09	–	–	–	–
Total	99.18	100.77	99.95	100.77	100.02	99.68	99.43	97.89	98.95	99.04	99.01	100.18	100.21
							atomic contents						
W	0.029	0.027	0.036	0.031	0.040	0.044	0.016	0.013	0.001	–	0.127	0.168	0.002
Nb	0.787	0.791	0.891	0.901	1.002	1.250	0.711	0.536	0.385	0.209	1.983	1.894	0.009
Ta	0.076	0.076	0.071	0.074	0.095	0.101	0.050	0.039	0.076	0.057	0.093	0.077	–
Ti	2.451	2.438	1.943	2.042	1.882	1.602	2.481	2.618	3.156	3.500	0.428	0.494	0.973
Zr	0.004	0.005	0.008	0.007	0.006	0.010	0.003	0.002	–	–	0.036	0.032	–
Sn	0.019	0.023	0.014	0.020	0.026	0.016	0.009	0.008	0.025	0.015	0.035	0.027	–
U	–	–	–	0.003	–	–	0.004	–	–	–	–	–	–
Sc	0.007	0.009	0.020	0.010	0.014	0.032	0.014	0.005	0.003	–	0.033	0.047	–
Y	–	0.001	0.001	–	–	–	–	–	–	–	0.003	–	–
Sb	0.001	–	–	–	–	–	–	0.002	–	–	–	–	–
Bi	–	0.001	–	–	–	–	–	0.002	–	0.01	–	0.002	–
Fe^{3+}	0.340	0.352	1.017	0.793	0.702	0.479	0.645	0.959	0.246	0.172	0.229	0.265	0.020
Fe^{2+}	0.281	0.275	0.935	1.076	1.165	1.375	1.785	1.466	0.107	0.041	0.999	0.990	0.980
Mn	0.001	0.002	0.061	0.042	0.063	0.085	0.275	0.345	–	0.003	0.032	0.004	0.015
Ca	–	0.001	–	–	0.002	0.001	0.003	0.003	–	–	0.001	–	–
Mg	–	–	0.001	–	–	0.002	0.003	–	–	–	–	–	0.001
Zn	0.004	–	–	–	–	–	–	–	–	0.003	–	–	–
Pb	–	–	–	–	–	–	–	0.002	0.001	–	–	–	–
Total	4.000	4.000	5.000	5.000	5.000	5.000	6.000	6.000	4.000	4.000	4.000	4.000	2.000

Notes: R = niobian rutile; PRI = Nb-poor pseudorutile I; PRII = Nb-rich pseudorutile II; PB = niobian ferropseudobrookite; RU = niobian rutile associated with titanian columbite; C = titanian columbite; – = below detection limit. R, RU, and C normalized to eight O atoms and four cations; PR to nine O atoms and five cations; PB to ten O atoms and six cations; ILM to three O atoms and two cations.

The rutile is compositionally homogeneous, with 37 to 43 at% of Ti substituted by other cations (R, Table 1). The Fe^{3+}/Fe^{2+} ratio is virtually constant at 1.2 to 1.3. Niobium strongly predominates over Ta, with Ta/(Ta+Nb) also constant between 0.07 and 0.09. The contents of W and Sn are subordinate, and those of Mn, Zn, Zr, and several other elements are negligible (Table 1). Unit-cell dimensions [a = 4.6384(8), c = 2.9883(7) Å] are distinctly higher than those of pure rutile (cf. Černý et al. 1964).

This rutile contains thin exsolution lamellae, 3 µm by 10 to 20 µm by 60 µm in size, apparently structurally controlled in their orientation and distribution (Figs. 2a and 2b). The composition of these lamellae yields satisfactory weight percent totals, cation contents, and integral stoichiometry when recalculated to five cations and nine O atoms. The ensuing formula corresponds to $Fe^{2+}Fe^{3+}(Nb,Ta)Ti_2O_9$, designated niobian pseudorutile I (PRI in Table 1).

PRI is preserved only in the thin tail-ends of the exsolution lamellae, whereas most of their volume is decomposed into a pair of new phases (Fig. 2b): Nb-rich pseudorutile II, which yields good weight percent totals and an integral sum of cations when normalized to nine oxygen atoms and five cations (PRII, Table 1; Fig. 3), and niobian-ferrian "ferropseudobrookite" based on ten oxygen atoms and 6 cations (PB, Table 1; Fig. 3).

PRII forms fine grains (1 to 3 µm across, bright in BSE images), hosted by niobian-ferrian "ferropseudobrookite" PB (dark in BSE); this latter phase also composes virtually single-phase seams central to the elongation of the lamellae (Fig. 2B). The overall ratio of the two minerals is approximately 1:1. Both pseudorutile PRII and "ferropseudobrookite" PB are slightly enriched in Mn relative to the pseudorutile PRI precursor; otherwise, they do not substantially differ in their (Ti,Sn):(Fe,Mn,Sc) ratios, but the proportion of (Nb,Ta) is distinctly different and is complementary relative to pseudorutile PRI (Figs. 3a and 3b).

Late advanced exsolution: Titanian ferrocolumbite and ilmenite

The rutile is further depleted in Fe, Mn, Nb, Ta, and W, and the bulk of the early assemblage reconstituted, during a massive exsolution into rutile + titanian ferrocolumbite + ilmenite (Fig. 2a). Parallel trains of ferrocolumbite micrograins are observed in poorly exsolved patches amidst fine-grained rutile + ferrocolumbite intergrowth, as textural relics after the early exsolution of pseudorutile and "ferropseudobrookite" (Fig. 4a). However, advanced coarse-grained stages of ferrocolumbite

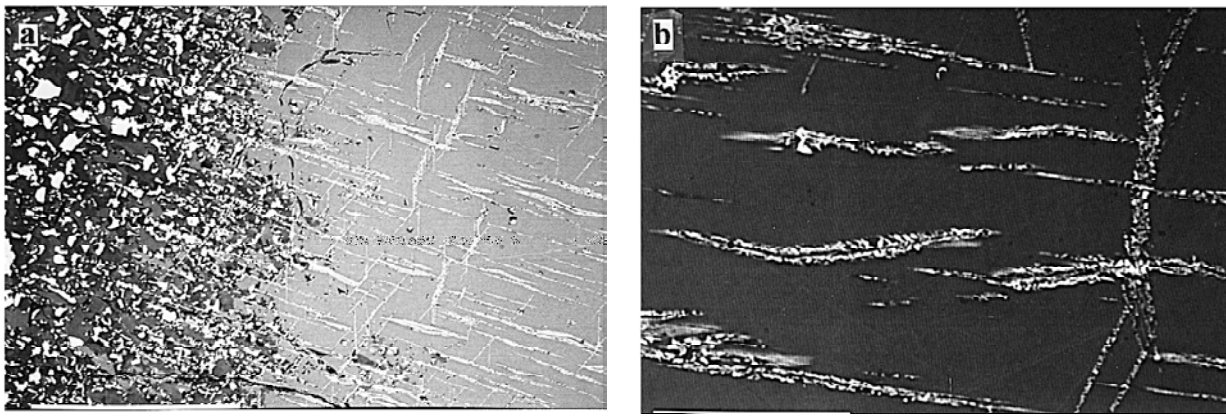

FIGURE 2. Exsolution in the McGuire niobian rutile in BSE images: **(a)** trellis-type pattern of niobian pseudorutile I (white) exsolved from niobian rutile (pale gray) on the right, and progressive exsolution of titanian ferrocolumbite (granular, white) from niobian rutile (progressively darkening) on the left side. The scale bar at the lower edge is 200 μm; **(b)** detail of the initial exsolution of niobian pseudorutile I from niobian rutile (black), with Nb-bearing pseudorutile I (gray) preserved only in the tail ends of the lamellae but otherwise exsolved into Nb-rich pseudorutile II (granular, white) imbedded in niobian-ferrian "ferropseudobrookite" matrix (black); Scale bar, 50 μm.

exsolution show randomly shaped and oriented grains of titanian ferrocolumbite with minor ilmenite in a compositionally heterogeneous and possibly somewhat recrystallized, granulated matrix of rutile (Fig. 4b).

Rutile RU is much more refined by the exsolution of titanian ferrocolumbite C than in the preceding stage (Table 1; Figs. 5a and 5b). Titanium is higher, whereas Nb, Zr, Sc, and total Fe are more depleted (Fig. 5b). Also, the Ta/(Ta+Nb) and Fe^{3+}/Fe^{2+} ratios (0.11 to 0.22 and 2.3 to 4.2, respectively) are higher than in the R compositions (Fig. 5a). The higher degree of exsolution is reflected in lower unit-cell dimensions of rutile, a = 4.6141(6) and c = 2.970(1) Å.

Identity of the exsolution product with titanian ferrocolumbite is suggested by its composition, which shows a moderate Ti content, Fe^{2+} dominant over Fe^{3+}, and low Sc (C in Table 1, Fig. 5). The identity is confirmed by structural characteristics: the essentially disordered natural ferrocolumbite with a = 4.712(1), b = 5.709(2), c = 5.111(2) Å becomes highly ordered upon heating to 1000 °C for 16 h in air, yielding an orthorhombic X-ray powder diffraction pattern with no wodginite-type maxima and parameters of a = 14.241(3), b = 5.720(2), and c = 5.508(2) Å (cf. Černý et al. 1998 for discrimination between titanian columbite and titanian ixiolite).

Composition of ilmenite is difficult to establish because of a rough polish of its somewhat skeletal grains (Fig. 4b). However, the available data leave no doubt about the identity of the mineral and its low content of Fe^{3+} and Mn (ILM in Table 1, Fig. 5b).

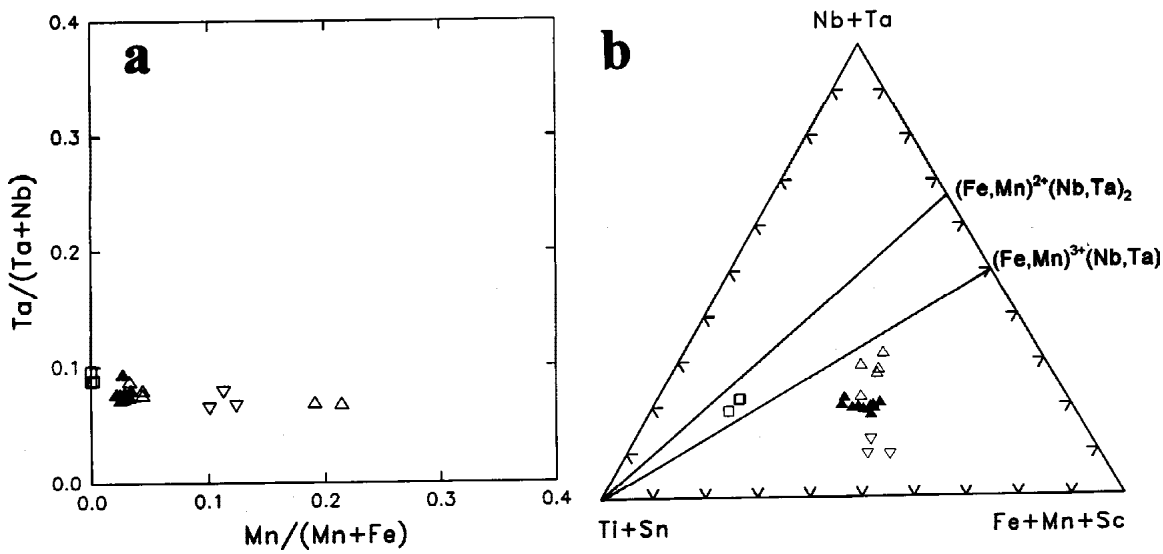

FIGURE 3. Early exsolution products of the primary McGuire niobian rutile. **(a)** The columbite quadrilateral (at. ratios). **(b)** The ternary (Nb+Ta) – (Ti+Sn) – (Fe+Mn+Sc) diagram (at%). Squares = niobian rutile matrix; solid triangles = Nb-bearing pseudorutile I; open triangles = Nb-rich pseudorutile II; inverted open triangles = niobian-ferrian "ferropseudobrookite."

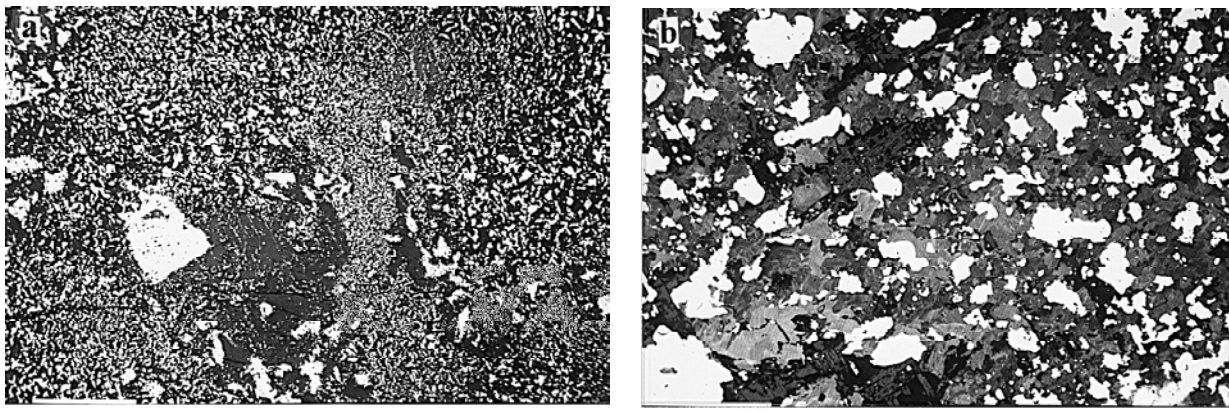

FIGURE 4. Advanced exsolution in the McGuire niobian rutile and reconstitution of its early exsolution products. **(a)** Fine-grained titanian ferrocolumbite (white) in niobian rutile (black); note the NNW-trending trains of fine ferrocolumbite grains, probably a textural relic after the early pseudorutile I, in the dark central patch of niobian rutile. **(b)** Coarser granular titanian ferrocolumbite (white) in compositionally heterogeneous granular niobian rutile (mottled gray), with three grains of ilmenite (dark gray, with NE-trending black streaks); the scale bars are 200 μm long.

Oxidation of niobian rutile

Subsequent to the exsolution of titanian columbite, niobian rutile is extensively replaced by skeletal aggregates of anatase with scattered interstitial micrograins and round or skeletal grains of a Nb,Ta-oxide mineral provisionally designated titanian ixiolite (Fig. 6). Interstices of the porous anatase rarely contain rounded relics of an iron-oxide phase, which cannot be accurately analyzed because of poor polish and rounded surface. However, the analytical results correspond to hematite rather than magnetite or any other potential Fe-oxide phase.

Anatase contains variable but subordinate Fe, Mn, Nb, and W, with no systematic mutual correlation (AR in Table 2; Fig 7a). Unit-cell dimensions of anatase a = 3.7845(2) and c = 9.5283(9) are barely above the values of compositionally pure samples (cf. Swanson and Tatge 1953).

Titanian ixiolite could not be separated, and in mixture with predominant anatase it did not yield X-ray powder diffractions sufficient for unambiguous interpretation and refinement of unit-cell dimensions. Thus, the name is only provisional but is suggested by the chemical composition (X in Table 2). High contents of Ti, W, Zr, and the high Fe^{3+}/Fe^{2+} ratio (1.36 to 1.60) compare well with those of titanian ixiolite (Černý et al. 1998b), and so far undefined $Fe^{3+}NbO_4$-dominant minerals (Ercit 1993; Uher et al. 1998; Černý et al. 1998a).

Oxidation of ilmenite

Coarse tabular ilmenite closely associated with niobian rutile locally shows compositions with near-ideal weight percent to-

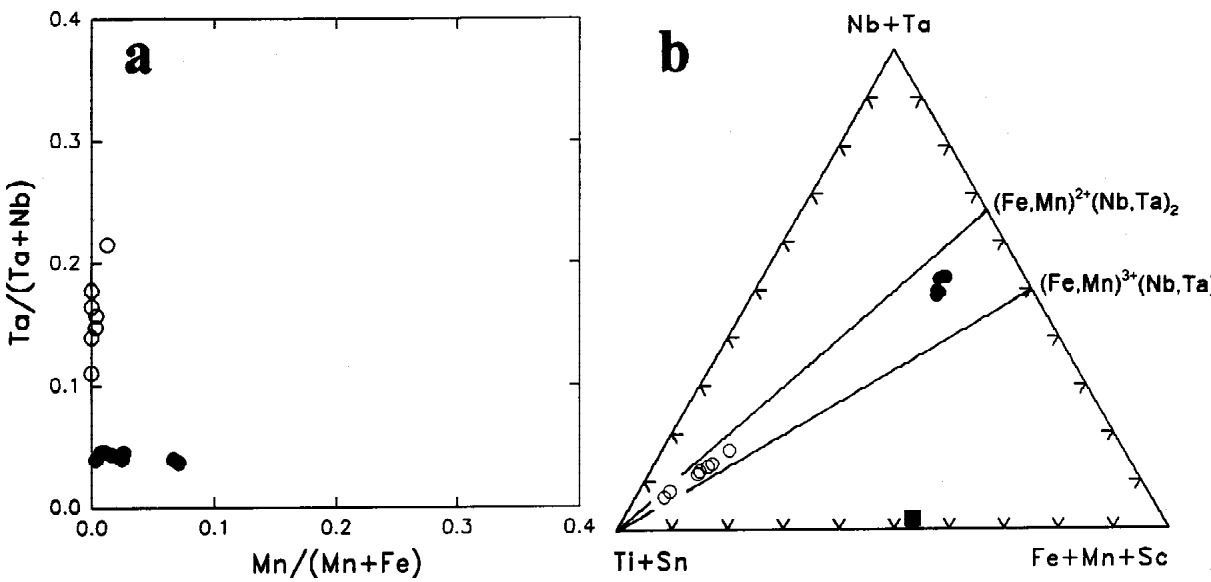

FIGURE 5. Products of late exsolution of the McGuire niobian rutile and reconstitution of its early exsolution products. **(a)** Columbite quadrilateral (at. ratios); **(b)** The ternary (Nb+Ta) – (Ti+Sn) – (Fe+Mn+Sc) diagram (at%). Open circles = depleted niobian rutile; solid dots = titanian ferrocolumbite; solid square = ilmenite.

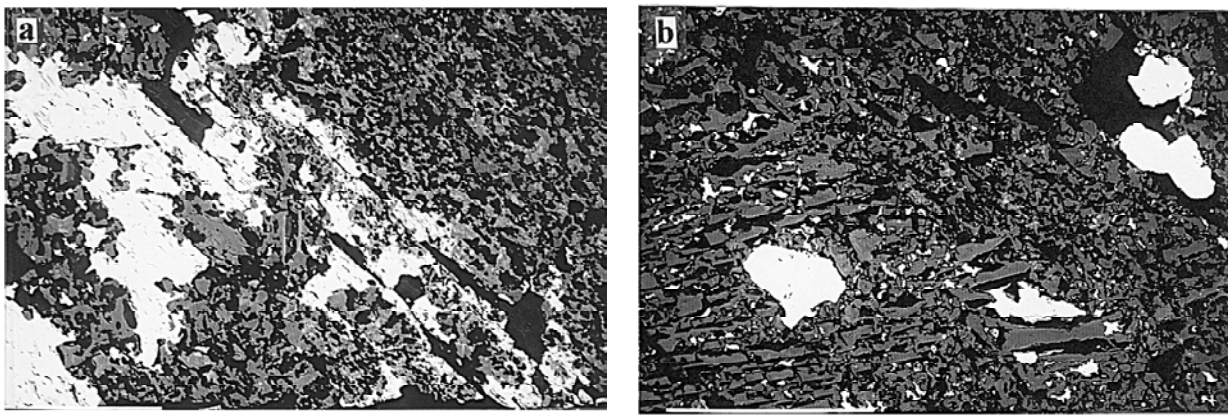

FIGURE 6. Oxidation of niobian rutile and its exsolution products in BSE images. **(a)** Dendritic titanian-tungstenian ixiolite (white) in a matrix of anatase (gray), highly porous (black) after leaching of hematite; the scale bar is 100 μm. **(b)** Round grains and minute anhedral specks of titanian-tungstenian ixiolite in the matrix of anatase (gray), with black pore space generated by leaching of hematite; the scale bar is 200 μm.

tals and stoichiometry, subordinate Mn, low Nb contents, and low calculated Fe^{3+} (IL in Table 2). This composition is apparently characteristic of the primary mineral, which can be seen on BSE images replaced by complex dendritic patches of slightly but significantly modified phases. Whereas the Nb content and, to a degree, that of Mn are maintained in other compositions, the proportions of Fe^{3+} and Fe^{2+} are highly variable, and so is the stoichiometry (Fig. 7b). Two kinds of deviations from the primary composition can be distinguished: ilmenite with higher Fe^{3+} (FIL in Table 2), and Fe^{3+}-free ilmenite depleted in Fe^{2+} and Mn (DIL in Table 2).

The Fe^{3+}-rich ilmenite FIL can be interpreted as resulting from incipient but pervasive oxidation of the primary phase; whereas, the DIL phase could have been produced by oxidation combined with leaching. Low weight percent totals and an apparent deficiency in A cations are characteristic of the DIL ilmenite normalized to two cations and three O atoms which suggests possible incorporation of $(OH)^-$. However, poor "dusty"-looking polish indicates extremely fine microporosity of this phase which may affect the results of electron-microprobe analysis. Consequently, crystal chemistry of this ilmenite cannot be unambiguously deciphered.

Replacement of ilmenite by fine-grained skeletal anatase with traces of rutile typically follows patches and "fronts" of Fe^{3+}-rich ilmenite. In accordance with the composition of its precursor, this anatase is low in Nb (Table 2, AI1 and AI2), but on average is higher in Fe than its counterpart which replaces niobian rutile (Fig. 7a). Poorly polished relics of a phase close to hematite are locally encountered in the pore space of the anatase aggregates. The pore space is more voluminous than that in skeletal anatase formed after niobian rutile.

DISCUSSION

Crystal chemistry

Niobian rutile. The chemical composition of the primary homogeneous niobian rutile, which is not preserved in the examined samples, was approximated by integrating the cation contents of the two phases resulting from early exsolution, niobian rutile R and pseudorutile PRI (the latter being representative of the sum of its own breakdown products, pseudorutile PRII and "ferropseudobrookite" PB). Image analysis yields ~12 vol% of the original pseudorutile I. As the unit-

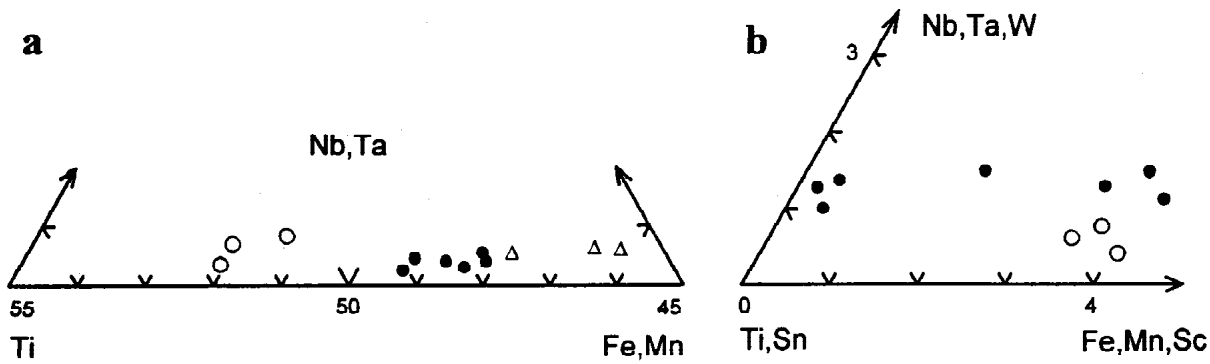

FIGURE 7. (a) Ilmenite in the Ti – (Nb,Ta) – (Fe,Mn) diagram (at%). Solid dots = primary ilmenite; triangles = oxidized secondary ferrian ilmenite; open circles = (Fe,Mn)-depleted ilmenite; **(b)** anatase in the (Ti,Sn) – (Nb,Ta,W) – (Fe,Mn,Sc) diagram (at%). Solid dots = anatase pseudomorphous after niobian rutile; open circles = anatase after ilmenite.

TABLE 2. Representative composition of ilmenite and oxidation products of ilmenite and niobian rutile

	IL1	FIL1	FIL2	DIL1	DIL2	AI1	AI2	AR1	AR2	IX1	IX2
WO_3	0.09	–	–	0.27	0.13	0.09	0.18	0.91	–	7.71	7.21
Nb_2O_5	0.93	1.07	1.25	1.37	1.20	0.94	0.53	8.77	2.24	45.30	46.20
Ta_2O_5	–	–	–	–	–	–	–	0.27	–	3.57	3.70
TiO_2	50.00	48.10	47.10	50.90	51.40	95.70	96.80	82.40	97.10	15.70	16.70
ZrO_2	–	–	–	–	–	–	–	–	–	1.01	0.95
SnO_2	–	–	–	–	0.05	–	0.02	0.18	–	1.30	1.37
UO_2	–	–	–	–	–	–	–	–	–	0.18	–
Sc_2O_3	–	–	–	–	–	0.02	–	–	0.01	0.62	0.63
Sb_2O_3	–	–	–	–	–	–	–	–	–	–	0.06
Bi_2O_3	–	–	–	–	0.11	0.15	–	–	–	–	–
Fe_2O_3	3.01	6.44	8.87	–	–	2.54	3.08	5.80	–	14.58	13.26
FeO	43.10	40.90	39.82	41.90	41.10	–	–	–	0.36	8.17	8.79
MnO	2.93	3.44	3.79	2.21	1.97	–	0.01	0.04	0.04	0.15	0.22
CaO	–	0.01	–	0.01	–	0.06	0.06	0.20	0.07	–	–
ZnO	–	–	–	–	0.05	–	–	–	–	–	–
PbO	–	0.05	0.08	0.20	–	0.12	0.06	0.11	0.13	–	–
Total	100.05	100.02	100.91	96.86	96.01	99.62	100.74	98.71	99.95	98.30	99.09
						atomic contents					
W	0.001	–	–	0.002	0.001	0.001	0.003	0.013	–	0.145	0.135
Nb	0.011	0.012	0.014	0.016	0.014	0.023	0.013	0.224	0.055	1.495	1.508
Ta	–	–	–	–	–	–	–	0.004	–	0.071	0.072
Ti	0.954	0.920	0.894	0.996	1.008	3.887	3.884	3.497	3.909	0.863	0.907
Zr	–	–	–	–	–	–	–	–	–	0.036	0.033
Sn	–	–	–	–	0.001	–	–	0.004	–	0.037	0.040
U	–	–	–	–	–	0.001	–	–	–	0.003	–
Sc	–	–	–	–	–	0.001	–	–	–	0.040	0.040
Sb	–	–	–	–	–	–	–	–	–	–	0.001
Bi	–	–	–	–	0.001	0.003	–	–	–	–	–
Fe^{3+}	0.057	0.123	0.168	–	–	0.104	0.124	0.247	–	0.801	0.720
Fe^{2+}	0.914	0.870	0.841	0.911	0.897	–	–	–	0.016	0.500	0.531
Mn	0.063	0.074	0.081	0.049	0.044	–	–	0.001	0.001	0.009	0.013
Ca	–	–	–	–	–	0.004	0.004	0.012	0.004	–	–
Zn	–	–	–	–	0.001	–	–	–	–	–	–
Pb	–	–	0.001	0.001	–	0.001	0.001	0.001	0.001	–	–
Total	2.000	2.000	2.000	1.976	1.966	4.025	4.029	4.003	3.986	4.000	4.000

Notes: IL1= primary ilmenite; FIL = partly oxidized ferrian ilmenite; DIL = $(Fe,Mn)^{2+}$-depleted ilmenite; AI = secondary anatase after ilmenite; AR = secondary anatase after niobian rutile; IX = secondary titanian ixiolite after niobian rutile; – = below detection limit. IL, FIL, and DIL normalized to three O atoms and two cations; AI, AR, and IX to eight O atoms and four cations.

cell volume and calculated density of pseudorutile PRI are not available, it is not possible to accurately calculate the composition of the primary homogeneous niobian rutile. Nevertheless, an approximation by reducing the cation total of pseudorutile PRI to four and combining cation contents of average rutile R and average pseudorutile PRI in a ratio of 88:12 lead to a formula of $(Ti_{2.34}Nb_{0.80}Ta_{0.07}W_{0.03}Sn_{0.02}Sc_{0.01}Fe^{3+}_{0.39}Fe^{2+}_{0.34})_{\sum 3.99}O_8$. This formula is not charge-balanced, having a deficit of 0.19 positive charges (1.2%) relative to 16 negative charges on oxygen. This suggests oxygen vacancies and/or $(OH)^-$ substitution; however, an excess of cations over four accomodated in interstitial sites seems to be more probable. This apparent imbalance is due to a slight excess of Fe^{2+} over the total (Fe^{2+}+Fe^{3+}) required to balance the incorporation of (Nb+Ta+W).

In contrast, the formula of depleted rutile R hosting the exsolved pseudorutile PRI is well balanced in terms of electrostatic charges and total Fe vs. (Nb+Ta+W): $(Ti_{2.44}Nb_{0.79}Ta_{0.08}W_{0.03}Sn_{0.02}Sc_{0.01}Fe^{3+}_{0.35}Fe^{2+}_{0.28})_{\sum 4.00}O_8$ (Table 1). The same applies to all individual compositions of rutile RU, which exsolved titanian ferrocolumbite C (Table 1). Although the formula of the homogeneous primary rutile is somewhat uncertain, the relative difference between its composition and those of R and RU phases can be discerned: the primary homogeneous rutile must have had an excess of Fe^{2+} over the columbite stoichiometry $A^{2+}B^{5+}$ to initially exsolve the Fe^{2+}-rich and Fe^{2+}-dominant pseudorutile PRI, and to exsolve minor ilmenite ILM along with titanian ferrocolumbite C in the second stage.

Fitting the composition of niobian rutile to the AO_2 stoichiometry and charge balance by adjusting the valences on Fe is the best routine approach to interpreting this mineral, but such treatment necessarily simplifies the issue of the crystal chemistry of this phase. A multitude of factors may modify the real constitution of rutile: interlayering with Fe_2O_3 (Hyde 1976; Putnis 1978), domain-scale intergrowth with goethite-type FeO(OH) layers (Grey et al. 1983), interstitial Fe^{3+} and other cations (Ruck et al. 1986; Smith and Persail 1997), oxygen deficiency (Noll 1949; Hyde 1976; Catlow and James 1982), cation vacancies (Putnis 1978), and incorporation of $(OH)^-$ paired in some cases with Fe^{3+} (Beran and Zemann 1971; Ruck et al. 1986, 1989, Hammer and Beran 1991; Vlassopoulos et al. 1993).

Pseudorutile I. The constitution of pseudorutile PRI seems to be well established as $(Fe,Mn)^{2+}(Fe,Sc)^{3+}(Nb,Ta)(Ti,Sn,Zr)_2O_9$ (Table 1). The required substitution $Fe^{2+}(Nb,Ta)^{5+}(Fe^{3+}Ti^{4+})_{-1}$ would be feasible from the crystal-chemical viewpoint, as both cations in the structures of pseudorutile (Grey et al. 1994) and synthetic $Fe^{3+}{}_2Ti_3O_9$ are octahedrally coordinated.

Pseudorutile II. This phase yields an average formula of $(Fe,Mn)^{2+}{}_{1.35}(Fe^{3+},Sc)_{0.61}(Nb,Ta,W)_{1.26}(Ti,Sn,Zr)_{1.77}O_9$. In view of the analytical difficulties in analyzing this extremely fine-grained phase and consequent broader margin of error, compliance of this phase with the formula of pseudorutile is not as good as in the case of pseudorutile I. However, the above for-

mula can be easily rounded off to $(Fe,Mn)^{2+}_{1.3}(Fe^{3+},Sc)_{0.7}(Nb,Ta)_{1.3}(Ti,Sn,Zr)_{1.7}O_9$, whereas recalculations to eight O atoms + four cations and ten O atoms + six cations give irrational numbers. This preferred formula also exhibits the $Fe^{2+}(Nb,Ta)^{5+}(Fe^{3+}Ti^{4+})_{-1}$ substitution. The formula is non-integral, but the substitution is more extensive than in the case of pseudorutile I.

Niobian "ferropseudobrookite." The composition of "ferropseudobrookite" PB given in Table 1, based on ten oxygen atoms and six cations (ap2fu), leads to an average formula of $(Fe,Mn)^{2+}_{1.93}(Fe^{3+},Sc)_{0.80}(Nb,Ta,W)_{0.68}(Ti,Sn,Zr)_{2.57}O_{10}$. This is the only acceptable interpretation, as recalculation to AO_2 stoichiometry gives non-integral results with Fe^{3+}only, and recasting to three O atoms and two cations eliminates Fe^{3+} and gives low weight percent totals yielding cation deficits. The only other normalization which yields formally tolerable results is to nine O atoms and five cations, with potentially acceptable weight percent totals and integral stoichiometry but $Fe^{3+} >> Fe^{2+}$. This last feature, however, cannot be accommodated by balanced exsolution. Uher et al. (1998) showed that a pseudobrookite-armalcolite phase exsolved from niobian rutile can contain appreciable Fe^{2+}, Mn and Nb, all substituting for Ti. In the present case, the phase in question can be interpreted as "ferropseudobrookite" with substantial substitution of $Fe^{3+}(Nb,Ta)Ti_{-2}$. The simplified formula for "ferropseudobrookite" PB is $Fe^{2+}_2(Ti_{2.6}Fe^{3+}_{0.7}Nb_{0.7})_{\Sigma 4.0}O_{10}$ for an ordered structure. The structure of pseudobrookite is well known for its flexibility in terms of alternative populations of cation sites, as well as for various degrees of high-temperature cation disorder (cf. review by Waychunas 1991), and metastable disorder may also be induced at low temperatures, aided by non-integral cation substitutions (Uher et al. 1998). All this makes the identification of niobian "ferropseudobrookite" quite plausible.

Titanian ferrocolumbite. The compositional and structural features of the titanian ferrocolumbite, given in the preceding descriptive sections, leave no doubt about its identity. The composition falls well within the range established by Černý et al. (1998).

Titanian-tungstenian ixiolite. This mineral could not be verified by X-ray diffraction of heated material, but its complex composition with high Ti, W, and Fe^{3+} contents strongly suggest that in a cation-ordered state it should have a wodginite-type or $Fe^{3+}NbO_4$-type structure, or it may break down to a mixture of both (cf. Ercit 1994; Černý et al. 1998).

Ilmenite. Ilmenite ILM produced during the exsolution of titanian ferrocolumbite from niobian rutile shows near-ideal stoichiometry with only minor cation substitutions. In contrast, the primary ilmenite IL1 displays subordinate hematite in solid solution, and its proportion increases with incipient oxidation in the FIL compositions (Table 2). The constitution of the product of this incipient invasive oxidation may be comparable to the ferrian ilmenite phase of Haggerty (1991), but we cannot satisfactorily interpret or find in the literature any analogs of the apparently A-depleted, ferroan DIL compositions (Table 2).

Pathway of the exsolution processes

The complete story of exsolution and breakdown of the McGuire niobian rutile is illustrated in Figure 8. The primary homogeneous niobian rutile initially broke down into a moderately (Fe,Mn,Nb,Ta)-depleted niobian rutile R with subordinate exsolution lamellae of niobian pseudorutile PRI. Structural control of this exsolution, apparent from the trellis-like lamellar pattern, is understandable in terms of the close structural relationship between rutile and pseudorutile. Both minerals share similar and commensurable cation arrangements in 001 planes within hexagonal close-packed anion layers (Grey and Reid 1975).

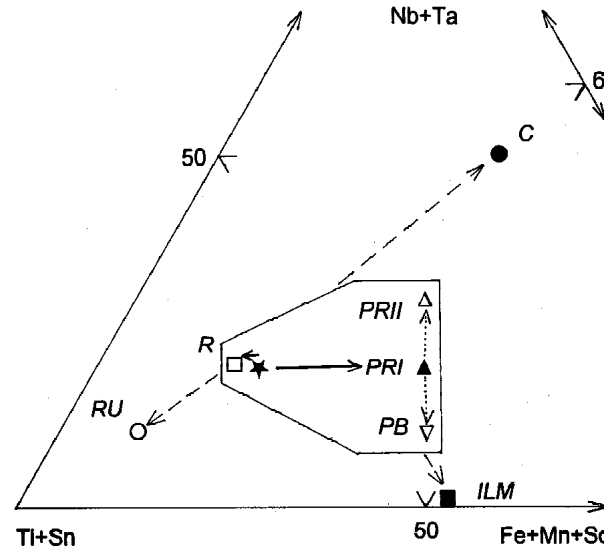

FIGURE 8. A summary diagram of exsolution processes in the McGuire niobian rutile; primary homogeneous niobian rutile marked by a star; acronyms of breakdown products as in Tables 1 and 2, graphic symbols as in Figures 3 and 5. The first, second, and third stages of exsolution and reconstitution are marked by solid, dotted, and dashed arrows, respectively.

The lamellar pseudorutile PRI decomposed into a (Fe^{3+},Nb)-rich derivative of niobian-ferrian "ferropseudobrookite" PB, studded by microgranular Nb-rich pseudorutile PRII. The "ferropseudobrookite" phase pseudomorphs the pseudorutile PRI lamellae, and it may also be in epitactic relation to the enclosing rutile; a close analogy was demonstrated for, e.g., pseudobrookite structure and rutile-goethite intergrowths (Grey et al. 1983).

The products of the above two processes are preserved only as local relics. The whole assemblage was subsequently overprinted by a wholesale exsolution and reconstitution that generated (Fe,Mn,Nb,Ta)-depleted niobian rutile RU with abundant titanian ferrocolumbite C and minor ilmenite ILM. These three minerals may represent a stable phase assemblage, but the broad compositional ranges of individual minerals show that they did not attain chemical equilibrium.

Exsolution products: Consistency in a closed system

Accurate modes of most of the secondary phases cannot be measured, particularly for the pseudorutile PRII and niobian-ferrian "ferropseudobrookite" PB, and for the niobian rutile RU + titanian ferrocolumbite C + ilmenite ILM assemblage. Precise quantitative treatment of the exsolution processes is consequently not possible. Nevertheless, at least a semiquantitative assessment is possible.

The (Nb,Ta,W) vs. (Fe,Mn) budget. The primary homogeneous niobian rutile was demonstrated to have contained a surplus of (Fe,Mn) over the quantity required for compensating the incorporation of (Nb,Ta,W) by the substitutions $(Fe^{2+},Mn)(Nb,Ta)_2Ti_{-3}$ or $Fe^{3+}(Nb,Ta)Ti_{-2}$, and minor $(Fe^{2+},Mn)WTi_{-2}$. This excess Fe was exsolved into the low-volume pseudorutile PRI with a high Fe/Nb ratio, and both pseudorutile PRI and the dominant rutile R become balanced in terms of the two substitutions above. The breakdown of pseudorutile PRI generates two phases, Nb-rich pseudorutile PRII and niobian-ferrian "ferropseudobrookite" PB, which are mutually complementary and maintain the balanced compensation of (Nb,Ta,W) by (Fe^{2+},Mn) and Fe^{3+} in their structures.

A third event transformed the bulk of all preexisting phases, which corresponds to the composition of the primary homogeneous niobian rutile characterized by excess Fe. The resulting depleted niobian rutile RU and titanian ferrocolumbite C show balanced Nb+Fe substitutions, and the excess Fe is accommodated in minor ilmenite ILM.

The Fe^{3+}/Fe^{2+} budget. The ferric/ferrous iron ratio is controlled by f_{O_2}. The primary assemblage of niobian rutile + ilmenite buffers f_{O_2} by the reaction $2Fe_2O_3$ (solid solution in ilmenite) + $4TiO_2 = 4FeTiO_3 + O_2$ (Zhao et al. 1998). Quantitative application of this equation is questionable at present, as the rutile contains 30 to 40% of $Fe^{2+}Nb_2O_6$ and $Fe^{3+}NbO_4$ combined, for which no a/X data are available. However, f_{O_2} must have been relatively low, below the NNO buffer, because the greatly reduced activities of TiO_2 in niobian rutile and of Fe_2O_3 in ilmenite.

The primary homogeneous niobian rutile had a Fe^{3+}/Fe^{2+} ratio close to 1.15. The initial exsolution generated mutually complementary phases, subordinate pseudorutile PRI (0.8 to 1.1) and dominant residual rutile R (1.2 to 1.3). Breakdown of pseudorutile PRI into Nb-rich pseudorutile PRII + niobian-ferrian "ferropseudobrookite" PB is again complementary in redistribution of the two irons; the Fe^{3+}/Fe^{2+} ratios are 0.35 to 0.60 and 1.5 to 3 in PRII and PB, respectively. The wholesale reconstitution of all preexisting phases, which can be represented by the Fe^{3+}/Fe^{2+} ratio 1.15 of the primary homogeneous niobian rutile, yields Fe^{3+}-enriched rutile RU (2.3 to 4.2), complemented by Fe^{2+}-dominated titanian columbite C (0.23 to 0.27) and ilmenite ILM (0.02).

Despite uncertainties about the precise composition of some minor phases and a lack of accurate data on modal compositions, the relationships discussed above suggest that all exsolution stages proceeded in a closed system. Throughout the whole process, the budget of (Nb,Ta) vs. (Fe,Mn) is consistent with the starting ratio calculated for the primary homogeneous niobian rutile. Similarly, the initial ratio of Fe^{3+}/Fe^{2+} seems to be maintained in the bulk of the breakdown products.

Exsolution in niobian rutile: control by Fe^{3+}/Fe^{2+} and Fe/Nb

Although the number of thoroughly documented cases is still small, it is becoming evident that the oxidation state of Fe in niobian rutile controls the nature of exsolved phases. In classic cases of highly Fe^{2+}-dominant rutile with (Nb,Ta) balanced by (Fe,Mn), titanian ferrocolumbite to manganocolumbite or titanian ixiolite are the only exsolution products (e.g., Černý et al. 1981). In (Fe^{3+},Sc)-dominant rutile with (Nb,Ta) balanced by (Fe,Mn), a titanian $(Fe^{3+},Sc)NbO_4$ phase with subordinate ferrocolumbite component is the only exsolution product (Černý et al. 1998). Niobian rutile with about equal amounts of Fe^{3+} and Fe^{2+} exsolves more complex and multistage mineral assemblages with individual phases showing different but complementary Fe^{3+}/Fe^{2+} ratios.

An imbalance in the (Fe,Mn) vs. (Nb,Ta,W) contents of rutile precursor also affects the nature of breakdown products. Uher et al. (1998) argued that pseudobrookite-armalcolite exsolved from the Pra šivá niobian rutile because of excess Fe over the columbite-type $A^{2+}B^{5+}$ ratio in the latter, and the same is true for the niobian pseudorutile and niobian-ferrian "ferropseudobrookite" here. Ilmenite identified in niobian rutile from Tesirogi (Černý et al. 1964; P. Uher and Černý, unpublished data) and ILM in the McGuire samples also attest to such excess of Fe in the parent niobian rutile.

Oxidation of the primary phases and exsolution products

The anatase + hematite + titanian ixiolite assemblage results from oxidation of niobian rutile and its exsolution products. The anatase + hematite assemblage that replaces primary ilmenite, closely following the initial oxidation front of ferrian ilmenite, was undoubtedly generated by the same oxidation event. Both assemblages subsequently suffered almost complete leaching of hematite. The overall effects are the same in both cases, with only two differences that are related to the constitution of the respective precursors. Fe^{3+}-rich titanian ixiolite is present only in the first assemblage, incorporating Nb, Ta, and W released from rutile and its breakdown products; these elements are minor in ilmenite. Also, the proportion of pore space after leached hematite is much higher in skeletal anatase after ilmenite than in its rutile-derived counterpart; this merely reflects the much higher content of Fe in ilmenite, and consequently higher percentage of hematite in its oxidation product.

The overall texture of the examined skeletal anatase with relics of hematite matches that of the anatase + hematite intergrowth, with preferred dissolution of the latter, resulting from oxidation of ilmenite in tropically weathered kimberlites (Haggerty 1991). In the absence of severe weathering in the Pikes Peak region, and in view of strong evidence of hydrothermal alteration of the host silicate assemblage in the McGuire pegmatite, we ascribe the oxidation of rutile and ilmenite to subsolidus pegmatite fluids at high f_{O_2}.

ACKNOWLEDGMENTS

This work was supported by the Natural Sciences and Engineering Research Council of Canada Major Installation, Equipment and Research Grants to P. Černý. The authors wish to acknowledge the constructive reviews by Greg Lumpkin and Eric Essene, which helped to eliminate several problems in interpretation and presentation.

REFERENCES CITED

Appleman, D.E. and Evans, H.T. Jr. (1973) Job 9214: indexing and least-squares refinement of powder diffraction data. U.S. Geological Survey, Computing Contributions, 20, NTIS Document PB2–16188.

Beran, A. and Zemann, J. (1971) Measurement of the infrared-pleochroism in minerals. XI. The pleochroism of the OH-stretching frequency in rutile, anatase, brookite and cassiterite. Tschermak's Mineralogische und Petrographische Mitteilungen, 15, 71–80.

Catlow, C.R.A. and James, R. (1982) Disorder in TiO_{2-x}. Proceedings of the Royal Society, London, A 384, 157–173.

Černý, P. and Ercit, T.S. (1985) Some recent advances in the mineralogy and geochemistry of Nb and Ta in rare-element granitic pegmatites. Bulletin de Minéralogie, 108, 499–532.

——— (1989) Mineralogy of niobium and tantalum: crystal chemical relationships, paragenetic aspects and their economic implications. In P. Moller, P. Cerny, and F. Saupé, Eds., Lanthanides, Tantalum and Niobium, 27–79. Springer-Verlag, Berlin Heidelberg.

Černý, P.,Čech, F., and Povondra, P. (1964) Review of ilmenorutile—strüverite minerals. Neues Jahrbuch für Mineralogie, Abhandlungen, 101, 142–172.

Černý, P., Paul, B.J., Hawthorne, F.C., and Chapman, R. (1981) A niobian rutile — disordered columbite intergrowth from the Huron Claim pegmatite, southeastern Manitoba. Canadian Mineralogist, 19, 541–548.

Černý, P., Goad, B.E., Hawthorne, F.C., and Chapman, R. (1986) Fractionation trends of the Nb- and Ta-bearing oxide minerals in the Greer Lake pegmatitic granite and its pegmatite aureole, southeastern Manitoba. American Mineralogist, 71, 501–517.

Černý, P., Ercit, T.S., Wise, M.A., and Buck, H.M. (1998) Compositional, structural and phase relationships in titanian ixiolite and titanian columbite-tantalite. Canadian Mineralogist, 36, 547–562.

Ercit, T.S. (1986) The simpsonite paragenesis; the crystal chemistry and geochemistry of extreme Ta fractionation. Unpublished Ph.D. thesis, University of Manitoba.

——— (1994) The geochemistry and crystal chemistry of columbite-group minerals from granitic pegmatites, southwestern Grenville Province. Canadian Mineralogist, 32, 421–438.

Ercit, T.S.,Černý, P., Hawthorne, F.C., and McCammon, C.A. (1992) The wodginite group. II. Crystal chemistry. Canadian Mineralogist, 30, 613–631.

Grey, I.E. and Reid, A.F. (1975) The structure of pseudorutile and its role in the natural alteration of ilmenite. American Mineralogist, 60, 898–906.

Grey, I.E., Li, C., and Watts, J.A. (1983) Hydrothermal synthesis of goethite-rutile intergrowth structures and their relationship to pseudorutile. American Mineralogist, 68, 981–988.

Grey, I.E., Watts, J.A. and Bayliss, P. (1994) Mineralogical nomenclature: pseudorutile revalidated and neotype given. Mineralogical Magazine, 58, 597–600.

Haggerty, S.E. (1991) Oxide textures—a mini-atlas. In Mineralogical Society of America Reviews in Mineralogy, 25, 129–219.

Hammer, V.M.F. and Beran, A. (1991) Variations in the OH concentration of rutiles from different geological environments. Mineralogy and Petrology, 45, 1–9.

Hyde, B.G. (1976) Rutile: planar defects and derived structures. In H.-R. Wenk, Ed.,Electron Microscopy in Mineralogy, 310–318. Springer-Verlag, Berlin Heidelberg.

Noll, W. (1949) Zür Kristallchemie des Zinnsteins (Kassiterit). Heidelberger Beiträge zür Mineralogie und Petrographie, 1, 593–625.

Novák, M. and Černý, P. (1998) Niobium-tantalum oxide minerals from complex pegmatites in the Moldanubicum, Czech Republic; primary versus secondary compositional trends. Canadian Mineralogist, 36, 659–672.

Putnis, A. (1978) The mechanism of exsolution of hematite from iron-bearing rutile. Physics and Chemistry of Minerals, 3, 183–197.

——— (1992) Introduction to mineral sciences, 457 p. Cambridge University Press, Cambridge, U.K.

Ruck, R., Babkine, J., Nguyen, C., Marnier, G., and Dusausoy, Y. (1986) Geochemical association of Fe and Nb in synthetic and natural cassiterites and rutiles. In Experimental Mineralogy and Geochemistry, Abstracts, Nancy, France, p.122–123.

Ruck, R., Dusausoy, Y., Nguyen Trung, C., Gaite, J.-M., and Murciego, A. (1989) Powder EPR study of natural cassiterites and synthetic SnO_2 doped with Fe, Ti, Na and Nb. European Journal of Mineralogy, 1, 343–352.

Sahama, T.G. (1978) Niobian rutile from Muiane, Mozambique. Jornal de Mineralogia Recife, 7, 115–118.

Simmons, W.B. and Heinrich, E.W. (1980) Rare-earth pegmatites of the South Platte district, Colorado. Colorado Geological Survey, Resource Series 11, 131 p.

Simmons, W.B., Lee, M.T., and Brewster, R.H. (1987) Geochemistry and evolution of the South Platte granite-pegmatite system, Jefferson County, Colorado. Geochimica et Cosmochimica Acta, 51, 455–471.

Smith, D.C. and Perseil, E.-A. (1997) Sb-rich rutile in the manganese concentrations at St. Marcel-Praborna, Aosta Valley, Italy: petrology and crystal chemistry. Mineralogical Magazine, 61, 655–669.

Swanson, H.E. and Tatge, E. (1953) Standard X-ray diffraction patterns. National Bureau of Standards, Circular 539, Vol. I.

Uher, P., Cerný, P., Chapman, R., Határ, J., and Miko, O. (1998) Evolution of Nb,Ta-oxide minerals in the Prašivá granitic pegmatites, Slovakia. I. Primary Fe,Ti-rich assemblage. Canadian Mineralogist, 36, 525–534.

Vlassopoulos, D., Rossman, G.R., and Haggerty, S.E. (1993) Coupled substitution of H and minor elements in rutile and the implications of high OH contents in Nb- and Cr-rich rutile from the upper mantle. American Mineralogist, 78, 1181–1191.

Waychunas, G.A. (1991) Crystal chemistry of oxides and oxyhydroxides. In Mineralogical Society of America Reviews in Mineralogy, 25, p. 11–68.

Zhao, D.-G., Essene, E.J., and Zhang, Y.-X. (1998) An oxygen barometer for rutile-ilmenite assemblages: oxidation state of metasomatic agents in the mantle. Earth and Planetary Science Letters, in press.

MANUSCRIPT RECEIVED AUGUST 10, 1998
MANUSCRIPT ACCEPTED JANUARY 12, 1999
PAPER HANDLED BY RODNEY C. EWING